THE JOURNAL OF BIOLOGICAL CHEMISTRY VOL. 286, NO. 47, pp. 41095–41104, November 25, 2011

Angiomotin-like2 Gene (*amotl2*) Is Required for Migration and Proliferation of Endothelial Cells during Angiogenesis*

Received for publication, August 22, 2011, and in revised form, September 20, 2011 Published, JBC Papers in Press, September 20, 2011, DOI 10.1074/jbc.M111.296806

Yeqi Wang[‡1], Zhiqiang Li[‡1], Pengfei Xu[‡], Lei Huang[‡], Jingyuan Tong[‡], Huizhe Huang[‡], and Anming Meng[‡§2]

From the [‡]State-key Laboratory of Biomembrane and Membrane Engineering, Tsinghua-Peking Center for Life Sciences, School of Life Sciences, Tsinghua University, Beijing 100084, China and the [§]Institute of Zoology, Chinese Academy of Sciences, Beijing 100101, China

Background: Amotl2 is expressed in blood vessels, but its function in vasculature formation is unknown.
Results: Amotl2 knockdown impairs intersegmental vessel growth in zebrafish embryos and *in vitro* tube formation of human endothelial cells.
Conclusion: Amotl2 is required for angiogenesis by regulating cell polarity, migration, and proliferation in a way related to MAPK activation.
Significance: Amotl2 plays important roles in regulating multiple behaviors of endothelial cells during angiogenesis.

Angiogenesis involves sprouting, migration, and proliferation of endothelial cells. The angiomotin-like2 gene (*amotl2*) has been found in blood vessels in zebrafish embryos, but its function in angiogenesis and underlying mechanisms remain unknown. In this study, we demonstrate that knockdown of *amotl2* in zebrafish *Tg(fli1:EGFP)^{y1}* and *Tg(fli1:nEGFP)^{y7}* transgenic embryos impairs the intersegmental vessel growth and suppresses proliferation of endothelial cells. Transplantation experiments indicate that function of *amotl2* in intersegmental vessel growth is cell-autonomous. *AMOTL2* knockdown in cultured human umbilical vein endothelial cells also inhibits cell proliferation and migration and disrupts cell polarity, ultimately interrupting the formation of vascular tube-like structures. Amotl2 promotes MAPK/ERK activation via c-Src, which is dependent on phosphorylation of tyrosine residue at position 103 but independent of the C-terminal PDZ-binding domain. Taking together, our data indicate that Amotl2 plays a pivotal role in polarity, migration and proliferation of angiogenic endothelial cells.

The first, primitive blood vessels in a vertebrate embryo are *de novo* formed through a process called vasculogenesis, from mesoderm-derived angioblasts. Thereafter, new blood vessels are formed predominantly through angiogenesis by sprouting of preexisting vessels. During angiogenesis, tip cell senses proangiogenic cues in the microenvironment with its numerous thin filopodia and then migrates toward a certain direction. One of the well studied angiogenic processes is the formation of dorsoventrally aligned intersegmental vessels (ISVs)[3] in the trunk of zebrafish embryos (1–4). During primary ISV formation, a pair of endothelial cells bilaterally exits the dorsal aorta at the position of the vertical somite boundary at approximately 20 h postfertilization (hpf). They grow dorsally along the somite boundary toward the dorsolateral roof of the neural tube. Because of proliferation of migrating endothelial cells, a primary intersegmental vessel upon arrival in the dorsal most position at 28–30 hpf usually consists of three to four cells (4, 5). The formation of intersegmental vessels is controlled by both intracellular factors and environmental cues.

The Motin protein family consists of three members, Angiomotin (Amot), Angiomotin-like1 (Amotl1), and Angiomotin-like2 (Amotl2) (6). Motin proteins have two coiled-coil domains and the C-terminal PDZ-binding motif in common and otherwise distinct domains. The founder member of this family, Amot, has been found to promote migration and tube formation of endothelial cells *in vitro* and *in vivo* (7–11). Amotl1 can also promote angiogenesis by controlling endothelial polarity and junction stability (12). We have demonstrated previously that *amotl2* expression in zebrafish embryos is positively regulated by FGF signals and required for gastrulation movements (13). Recently, all Motin family members have been shown to associate with YAP or TAZ, members of the Hippo pathway, and act to retain them in the cytoplasm (14–16).

The extracellular signal-regulated kinases (ERKs) are activated by growth factors and other extracellular cues and play important roles in cell proliferation, cell migration, organogenesis, and tumorigenesis (17). *ERK2* knock-out mouse embryos are lethal with few fetal blood vessels, suggesting an essential role in angiogenesis (18). ERK-mediated FGF and VEGF signaling pathways have been found to possess proangiogenic activity in normal and pathological tissues (19–22). Recently, Yi *et al.* demonstrated that Amot is a positive regulator of Rac1/MAPK/ERK signaling in HEK293 cells and *Nf2*$^{-/-}$ Schwann cells (23), whereas Wang *et al.* found that Amotl2 negatively regulates ERK activation in MCF10A cells (15). It is likely that different Motin members have distinct functions in regulating MAPK/

* This work was supported by Major Science Programs of China Grants 2011CB943800 and 2012CB945101 and by National Natural Science Foundation of China Grant 30921004/C061003.
[1] Both authors contributed equally to this work.
[2] To whom correspondence should be addressed. Tel.: 86-10-62772256; Fax: 86-10-62794401; E-mail: mengam@mail.tsinghua.edu.cn or mengam@ioz.ac.cn.
[3] The abbreviations used are: ISV, intersegmental vessel; Amotl2, Angiomotin-like2; DLAV, dorsal longitudinal anastomotic vessel; hpf, hours postfertilization; HUVEC, human umbilical vein endothelial cell; MO, morpholino; PLCγ1, phospholipase Cγ1; PP2, 4-amino-5-(4-chlorophenyl)-7-(*t*-butyl)pyrazolo[3,4-d]pyrimidine.

ERK signaling or a Motin member acts differently depending on cell types or cellular processes.

The expression of *amotl2* also occurs in axial vasculature and intersegmental vessels during pharyngula stages in zebrafish embryos (13). However, implication of Amotl2 in blood vessel formation has not been reported in any species. In this study, we demonstrate that zebrafish *amotl2* is required for ISV growth, and proangiogenic activity of Amotl2 is conserved in cultured human umbilical vein endothelial cells (HUVECs). Amotl2 is required for ERK activation in endothelial cells.

EXPERIMENTAL PROCEDURES

Zebrafish and Embryonic Manipulations—*Tg(fli1:EGFP)^{y1}* (3) and *Tg(fli1:nEGFP)^{y7}* (5) transgenic lines were used. Embryos were raised in Holtfreter solution at 28.5 °C. Ethical approval was obtained from the Animal Care and Use Committee of Tsinghua University. Capped RNAs (mRNAs) were synthesized using T7 mMessage Machine kit (Ambion) according to the manufacturer's instructions. The morpholino amotl2-MO1 (5′-CTGATGATTCCTCTGCCGTTCTCAT-3′) and its control amotl2-cMO1 (its sequence was derived from the amotl2-MO1 sequence) were described previously (13). Synthetic mRNAs and morpholinos were injected into zebrafish embryos at the one-cell stage. The coding sequence of *amotl2^{m}* started with ATGCGTACCGCTGAAGAGAGCTCA, which contained mutated bases (underlined) and could not be bound by amotl2-MO1. The injection doses were given in corresponding places. For cell transplantation, *Tg(fli1:EGFP)^{y1}* embryos were injected at the one-cell stage with 20 ng of dextran tetramethylrhodamine (Molecular Probes) alone or in combination with amotl2-MO1 and used as donors at the sphere stage (about 4 hpf). When needed, host embryos were injected with amotl2-MO1 at the one-cell stage. Cell transplantation was done as before (24), and embryos were observed at 30–32 hpf.

Cell Culture, Luciferase Assay, and Immunoblotting—HEK293T cells and HUVECs were grown in DMEM (Invitrogen) supplemented with 10% FCS (Hyclone). When stimulation was required, the cells were starved for 18 h and then treated with 20 ng/ml FGF2 (Sigma). At 48 h after transfection with the ERK reporter ELK-luciferase, cells were harvested with passive lysis buffer (Promega, Madison, WI), and luciferase activity was then measured using a luminometer (Berthold Technologies, Oak Ridge, TN). Transfection efficiency was normalized by *Renilla*. For chemical treatments, cells were serum-deprived for 2 h and then treated with 20 μM PP2 (Src inhibitor from Calbiochem) or 10 μM U5402 (FGFR1 inhibitor from Calbiochem) for 2 h at 37 °C prior to FGF2 stimulation. Western blotting and immunoprecipitation were then performed as before (25). For detection of ERK1/2 or p-ERK1/2 levels in embryos, embryos at 30 hpf were harvested for Western blotting as before (26). Antibodies for Western blotting were as follows: anti-p-ERK (E-4) mAb, anti-HA (F-7) mAb, anti-Myc (9E10) mAb, anti-GFP mAb, anti-pAKT1/2/3 polyclonal antibody, anti-pPLCγ1 mAb, anti-ERK1/2 polyclonal antibody, anti-AKT1/2/3 polyclonal antibody, and anti-pPLCγ1 polyclonal antibody from Santa Cruz; anti-Tyr(P) (6D12) monoclonal antibody from MBL; and the secondary antibodies from Jackson ImmunoResearch Laboratories.

AMOTL2 Knockdown in Human Cells—*AMOTL2* shRNA was synthesized to target the sequence 5′-GGAGATGGAAAGCAGGTTAAA-3′ of human *AMOTL2* by GenePharma Co., and the scrambled control shRNA was obtained from the same company. For the tube formation, cell proliferation, and wound healing assays, *AMOTL2* shRNA or the control shRNA was subcloned into the modified lentiviral vector pLL3.7. Viruses were produced by transfecting HEK293T cells with corresponding shRNA lentiviral construct and the viral packaging vectors (psPAX2, pMD2G) by calcium phosphate transfection and harvested from the supernatant 48 h after transfection. For the other assays, *AMOTL2* or control shRNA was cloned into the plasmid vector pGPU6/GFP/Neo. The efficiency of *AMOTL2* knockdown was tested in HEK293T cells by analyzing *AMOTL2* transcript levels via RT-PCR and by examining expression levels of co-transfected Myc-AMOTL2 by Western blotting.

In Vitro Tube Formation, Wound Healing, and Proliferation Assays—For tube formation assay, 12-well plates were coated with 200 μl/well growth factor-free Matrigel (BD Biosciences). HUVECs (2×10^5 cells/well) were infected with shRNA-expressing viruses with a $TCID_{50}$ of 5×10^6, and then seeded and cultured for 16 h in DMEM. The length of formed tubes was measured. For the wound healing assay, HUVECs cells seeded in 60-mm dishes were infected with shRNA-expressing viruses and grown to 90% confluence. The cells were then starved for 12 h in DMEM containing 0.3% FCS. A wound was made with a 100-μl pipette tip, and cells were observed 48 h later. For proliferation assay, 50,000 shRNA-expressing HUVECs were seeded onto 25-mm dishes and starved for 12 h with DMEM containing 0.3% FCS, and the cell number was counted 48 h after starvation.

RESULTS

amotl2 Knockdown Impairs Growth of Intersegmental Vessels—We have showed previously that zebrafish *amotl2* is expressed in the dorsal aorta, posterior cardinal vein, and ISVs at pharyngula stages (13). In our previous study, we demonstrated that *amotl2* expression could be effectively inhibited by injection of a specific antisense morpholino (amotl2-MO1), and *amotl2* knockdown caused defective gastrulation cell movements in a dose- dependent manner (13). To investigate the effect of *amotl2* knockdown on angiogenesis, we used *Tg(fli1:EGFP)^{y1}* transgenic line, which expresses EGFP in the whole vasculature (3). We first titrated amotl2-MO1 to a high dose that would not cause obvious gastrulation defects. As shown in Fig. 1, epibolic progression of embryos injected with 1.5 or 2.5 ng of amotl2-MO1 was comparable with that of uninjected wild-type embryos or embryos injected with 3 ng of control MO (amotl2-cMO1); at 30 hpf, amotl2-MO1-injected embryos did not show a general developmental delay or other severe morphological defects (Fig. 1*B*). Therefore, injection of amotl2-MO1 at or below 2.5 ng/embryo could be appropriate for investigating *amotl2* knockdown effect on angiogenesis.

For easier characterization, we paid attention to observing ISV growth after amotl2-MO1 injection. As observed at 30 hpf, the ISVs in uninjected or amotl2-cMO1-injected *Tg(fli1:EGFP)^{y1}* embryos uniformly reached the dorsolateral roof of

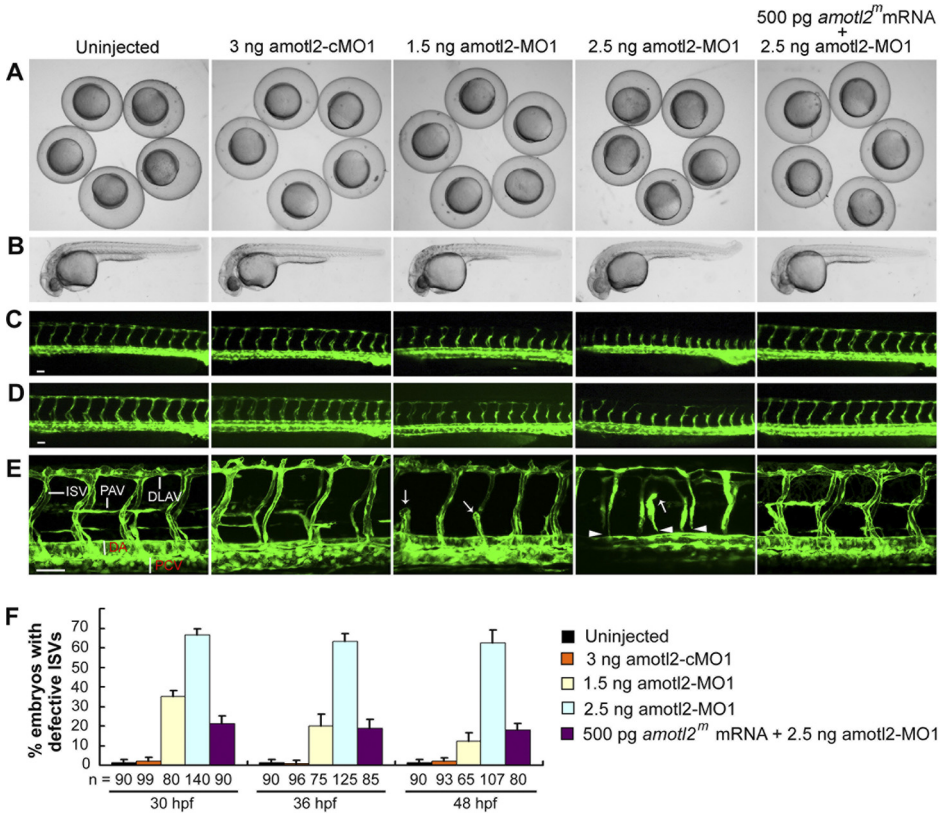

FIGURE 1. ***amotl2* knockdown impairs intersegmental vessel growth in zebrafish embryos.** *A* and *B*, *bright filled* images showing gross morphology of uninjected or injected *Tg(fli1:EGFP)*^{y1} embryos at different stages. Injections were performed at the one-cell stage. Note that injected embryos generally showed a normal morphology. *C–E*, fluorescent images showing ISVs of *Tg(fli1:EGFP)*^{y1} embryos at the indicated stages. Embryos were orientated with anterior to the *left*. Note that ISVs in *amotl2* morphant grew far behind those in uninjected or amotl2-cMO1-injected controls at 30 and 36 hpf. In morphants at 48 hpf, halted ISVs are indicated by *arrows*; ISVs inappropriately connected with the dorsal aorta are indicated by *arrowheads*. *PAV*, parachordal vessel. *Scale bar*, 75 μm in *C* and *D*, 50 μm in *E*. *F*, percentage of embryos with defective ISVs at different stages. The number of analyzed embryos (*n*) is indicated. *Error bars*, S.D.

the neural tube (Fig. 1*C*); in contrast, the majority of the ISVs in the affected morphants did not grow to a similar position. At 36 hpf, the ISVs in the control embryos had fully joined to form the dorsal longitudinal anastomotic vessels (DLAVs) (Fig. 1*D*), whereas in the morphants some ISVs had not arrived in the dorsal most position, and DLAV formation was incomplete. At 48 hpf in the control embryos, an interconnected luminal pathway from the dorsal aorta to the DLAV had been established, and parachordal vessels were forming; but in the morphants, some ISVs still halted on the half way (indicated by *arrows*), parachordal vessels were absent, and lumens of some vessels were abnormal (Fig. 1*E*). Generally, defects in embryos injected with 2.5 ng of amotl2-MO1 were more severe than those injected with 1.5 ng of amotl2-MO1. Importantly, the ISV defects of the morphants could be rescued by co-injection of 500 pg of *amotl2*^{m} mRNA (Fig. 1), a mutant form that could not be bound by amotl2-MO1 (13). These results suggest that *amotl2* is essential for the formation of ISVs in zebrafish embryos.

amotl2 Is Required for ISV Growth in a Cell-autonomous Fashion—To test whether implication of *amotl2* in ISV growth is cell-autonomous, we performed cell transplantation experiments using *Tg(fli1:EGFP)*^{y1} blastula cells as donor cells and wild-type embryos as hosts. The transplanted cells in 41.7% (n = 72) of host embryos grew out an average of 2.9 EGFP-positive ISVs at 30–32 hpf, which had arrived at the dorsolateral roof of the neural tube (Fig. 2, *A-C*). When donor cells were taken from amotl2-MO1-injected *Tg(fli1:EGFP)*^{y1} blastulas, these cells in most (86.7%, n = 90) of host embryos failed to form any EGFP-positive ISVs as observed at 30–32 hpf (see Fig. 2, *D–F*, for an example); and in case that EGFP-positive ISVs (1.4 on average) appeared, they usually did not reach the neural tube roof position (see Fig. 2, *G–I*, for an example). These results indicate that cells depleted of *amotl2* hardly contributed to the ISVs in normal environments, suggesting a cell-autonomous requirement of *amotl2* for angiogenesis. When embryonic cells from *Tg(fli1:EGFP)*^{y1} embryos were transplanted into amotl2-MO1-injected host embryos, 34.2% of the hosts (n = 76) had an average of 2.6 EGFP-positive ISVs (see Fig. 2, *J–L*, for an example), suggesting that the availability of Amotl2 in endothelial cells is more important for angiogenesis than Amotl2 expressed in nonendothelial cells.

amotl2 Knockdown Inhibits Proliferation of ISV Endothelial Cells—It has been found that endothelial cells of ISVs in zebrafish embryos can proliferate as they migrate (5, 27). We then asked whether *amotl2* is also required for the proliferation of the ISV endothelial cells. To address this issue, we used *Tg(fli1:nEGFP)*^{y7} transgenic embryos, which express EGFP in the nuclei of endothelial cells (5). At each time point, a total of 30 embryos for each group and 10 ISVs/embryo were observed under a fluorescence microscope to count the number of nuclei (Fig. 3, *A–D*). In amotl2-cMO1 (3 ng)-injected embryos, the

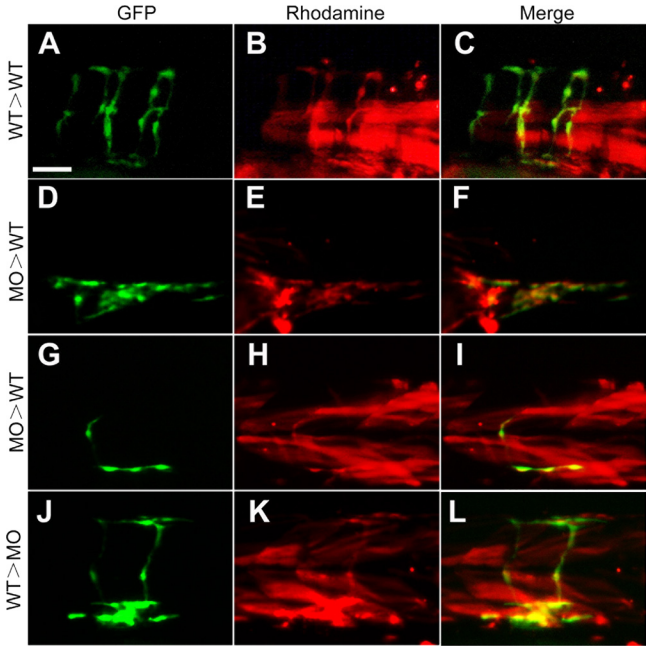

FIGURE 2. ***amotl2* is required for intersegmental vessel growth in a cell-autonomous fashion.** Donor *Tg(fli1:EGFP)*^{y1} embryos were injected with dextran tetramethylrhodamine (*red*) at the one-cell stage, and cells were taken at the sphere stage and transplanted into a stage-matched host embryo. Host embryos were observed for GFP-expressing ISVs by confocal microscopy at 30 hpf. *A–C*, uninjected donor cells could grow out ISVs in wild-type host embryos. *D–I*, donor cells injected with 1.5 ng of amotl2-MO hardly generated ISVs in most cases (*D–F*) or formed a few ISVs occasionally (*G–I*) in wild-type host embryos. *J–L*, uninjected donor cells could grow out ISVs in amotl2-MO1 (1.5 ng)-injected host embryos. *Scale bar*, 75 μm.

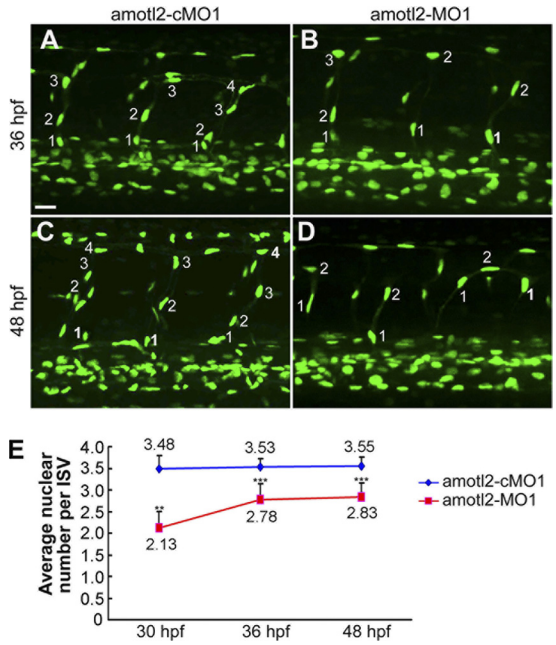

FIGURE 3. ***Amotl2* knockdown inhibits proliferation of endothelial cells of ISVs in zebrafish embryos.** *A–D*, confocal images showed distribution of endothelial cell nuclei in *Tg(fli1:nEGFP)*^{y7} embryos at different stages. Injection doses were 3 ng for amotl2-cMO1 and 2.5 ng for amotl2-MO1. The nuclei of ISVs located on one trunk side were numbered in sprouting and dividing orders. Only nuclei located between DLAV and dorsal aorta were counted. Embryos were placed with anterior to the left and dorsal to the top. *E*, statistical analysis of nuclear number/ISV. 30 embryos and 10 ISVs per embryo were analyzed for each group. **, $p < 0.001$; ***, $p < 0.01$. *Error bars*, S.D.

average number of nuclei/ISV was 2.48, 3.53, and 3.55 at 30, 36, and 48 hpf, respectively. In contrast, in amotl2-MO1 (2.5 ng)-injected embryos, the average number was 2.13, 2.78, and 2.83 at 30, 36, and 48 hpf, respectively. Because the number of ISV endothelial cells in *amotl2* morphants at 48 hpf was still much less than that in control embryos, amotl2-MO1-induced reduction of ISV endothelial number may not be caused by delay of proliferation. The prohibited proliferation of ISV endothelial cells is likely to be one of the mechanisms for abnormal growth of ISVs in *amotl2* morphants.

AMOTL2 Knockdown Affects Tube Formation, Migration, Proliferation, and Polarity of HUVECs—To test the conservation of angiogenic activity of *Amotl2*, we performed a vascular tube formation assay using HUVECs. The expression of *AMOTL2* was markedly reduced by *AMOTL2* shRNA (Fig. 4 , *A* and *B*), indicative of efficient knockdown. The HUVECs expressing scrambled shRNA (control shRNA) were able to form a tube-like structure (Fig. 4*C*). When infected with viruses expressing *AMOTL2* shRNA, however, the tube formation of the HUVECs was perturbed (Fig. 4, *C* and *D*). It is apparent that *AMOTL2* is required for *in vitro* tube formation of human endothelial cells.

In a wound healing assay using HUVECs, the wound in cell culture depleted of *AMOTL2* healed more slowly compared with the wound in cells expressing scrambled shRNA (Fig. 4, *E* and *F*), suggesting a requirement of AMOTL2 for endothelial cell migration. Like in zebrafish embryos, the proliferation of HUVECs was also inhibited by *AMOTL2* knockdown (Fig. 4*G*). We investigated whether *AMOTL2* knockdown could disrupt HUVEC polarization by examining the location of the Golgi apparatus. As reported previously by others (10, 12, 28), the Golgi apparatus in HUVECs transfected with the scrambled shRNA plasmid, which was immunostained using a TGN46 Golgi antibody, was uniformly located within an 120° sector relative to the nucleus in the direction of migration (Fig. 4*H*, *left*). In contrast to 96.3% of scrambled shRNA-transfected cells ($n = 54$) with normal Golgi apparatus location, 30.4% of cells expressing *AMOTL2* shRNA ($n = 69$) showed scattered distribution of TGN46-positive vesicles (Fig. 4, *H* and *I*), suggesting that *AMOTL2* plays a role in acquiring endothelial polarization. Taken together, the above results suggest that Amotl2 participates in angiogenesis by controlling polarity, proliferation, and migration of endothelial cells.

Amotl2 Is Required for MAPK/ERK Activation during Angiogenesis—Previous studies have demonstrated that MAPK/ERK signaling is required for angiogenesis (29) and that Motin members may regulate MAPK/ERK activation in cultured cells (15, 23). We asked whether Amotl2 function in angiogenesis is related to MAPK/ERK activation. To address this question, we first injected amotl2-cMO1, amotl2-MO1, or *amotl2*^{m} mRNA into wild-type one-cell embryos and examined by Western blotting total and phosphorylated ERK levels at 30 hpf (Fig. 5, *A* and *B*). amotl2-MO1 injection led to obvious reduction of p-ERK levels in a dose-dependent manner, whereas the total cellular ERK levels were unaltered. Injection with amotl2-cMO1 had no effect on either p-ERK or total ERK levels. Overexpression of amotl2 by *amotl2*^{m} mRNA injection caused an increase of p-ERK by about 25%. Importantly, p-ERK

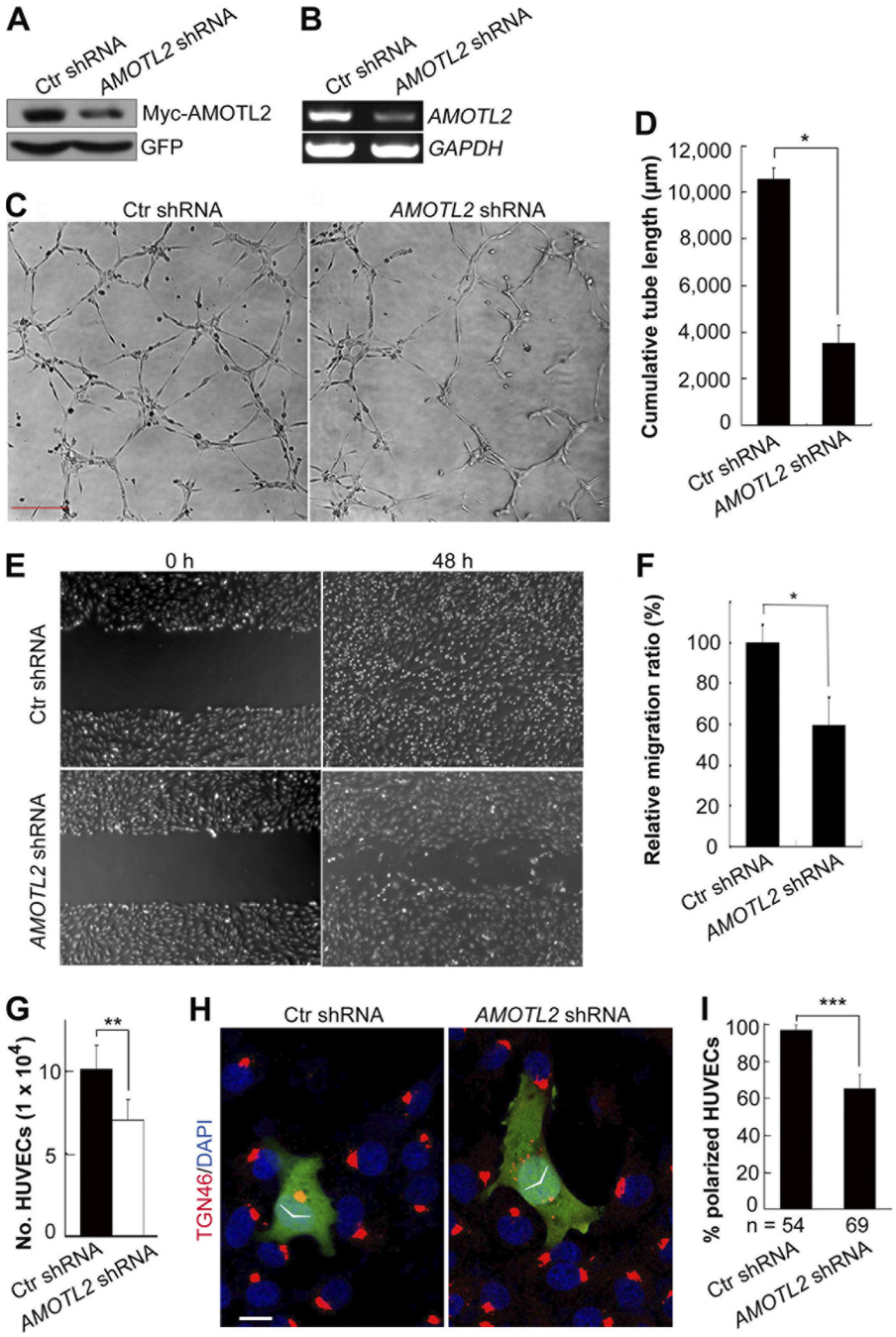

FIGURE 4. ***AMOTL2* is required for proliferation, migration, polarity, and tube formation of human endothelial cells.** *A*, transfection of *AMOTL2* shRNA efficiently blocked expression of co-transfected Myc-AMOTL2 in HEK293T cells. pCMV-EGFP was also co-transfected. Myc-AMOTL2 and GFP were examined by Western blotting using anti-Myc and anti-GFP antibodies, respectively. *B*, transfection of *AMOTL2* shRNA efficiently reduced endogenous *AMOTL2* transcripts in HEK293T cells as examined by RT-PCR. *GAPDH* served as a control. *C*, vascular tube-like structures were formed by HUVECs expressing control or *AMOTL2* shRNA in Matrigel. *Scale bar*, 100 μm. *D*, cumulative tube length per field was compared. *, $p < 0.05$. *Error bars*, S.D. *E* and *F*, wound-healing behavior of HUVECs expressing control or *AMOTL2* shRNA is shown. The relative migration ratio was compared (*F*). *, $p < 0.05$. *G*, the number of HUVECs expressing different shRNAs was compared after culture for a defined period. **, $p < 0.01$. *H* and *I*, the subcellular location of the Golgi apparatus in HUVECs transfected with control or *AMOTL2* shRNA is shown. Cells were immunostained with anti-TGN46 antibody, and nuclei were labeled with DAPI. Statistical data are shown in *I*.

reduction by amotl2-MO1 could be recovered by co-injection of *amotl2*^{m} mRNA. These results imply that the activation of MAPK signaling in zebrafish embryos requires Amotl2 function.

Next, we examined p-ERK levels in the ISVs by immunostaining of transverse sections of *Tg(fli1:EGFP)*^{y1} transgenic embryos at 30 hpf using the anti-p-ERK antibody. As shown in Fig. 5*C*, p-ERK levels in an ISV of an amotl2-MO1-injected embryo were lower compared with those in the amotl2-cMO1-injected embryo. Thus, the ERK activation in ISVs is dependent on Amotl2 activity.

To understand better the selectivity of Amotl2 action on ERK activation, we tested effects of human *AMOTL2* overexpression on different pathways downstream of FGF signals in HEK293T cells. *AMOTL2* overexpression enhanced p-ERK1/2 activation and extended the duration of FGF2-induced ERK1/2 phosphor-

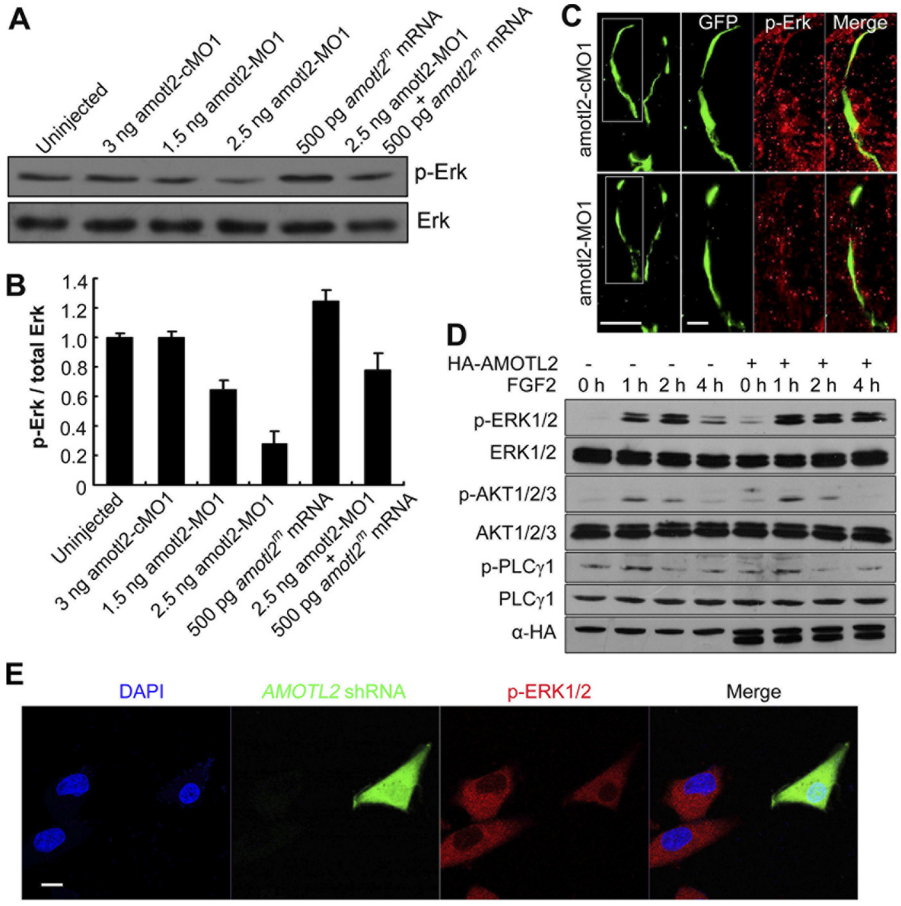

FIGURE 5. **Amotl2 positively regulates MAPK/ERK activation.** *A* and *B*, *amotl2* knockdown in zebrafish embryos reduced p-ERK levels. Embryos were injected at the one-cell stage with the indicated morpholino and/or mRNA and harvested at 30 hpf for Western blotting using anti-p-ERK or anti-ERK antibody. The relative p-ERK levels were compared by densitometric analysis from three independent experiments (*B*). *Error bars*, S.D. *C*, p-ERK levels were examined by immunostaining cryosections of *Tg(fli1:EGFP)*^{y1} transgenic embryos in the trunk region at 30 hpf using anti-p-ERK and anti-GFP antibodies. The *boxed areas* in the *left column* are enlarged in the *right columns*. *Scale bars*, 20 μm. *D*, AMOTL2 enhanced ERK activation but not AKT1/2/3 or PLCγ1 activation in HEK293T cells. Protein levels were detected by Western blotting using corresponding antibodies. *E*, p-ERK1/2 level in HUVECs expressing *AMOTL2* shRNA was reduced. 24 h after transfection, the cells were starved for 16 h and then were stimulated for 15 min with 20 ng/ml FGF2. Endogenous p-ERK1/2 was examined by immunostaining using an anti-p-ERK antibody. *Scale bar*, 20 μm.

ylation (Fig. 5*D*). However, *AMOTL2* overexpression showed little effect on the phosphorylation of Akt1/2/3 and PLCγ1 (Fig. 5*D*), both of which have been previously found to be activated by FGF signals (30). Furthermore, FGF2-stimulated ERK1/2 phosphorylation in HUVECs was reduced by *AMOTL2* knockdown (Fig. 5*E*). These results provide a piece of evidence that Amotl2 selectively promotes FGF-induced MAPK activity.

Amotl2-promoted MAPK Activation and Endothelial Proliferation Are Independent of PDZ-binding Motif—The conserved C-terminal PDZ-binding motif of the Motin family members is critical for regulating cell polarity and movements, and the mutant forms lacking this motif have a dominant negative effect on corresponding wild-type proteins (7, 8, 13, 31). We wondered whether this motif plays a role in Amotl2-promoted MAPK activation. We found that, like zebrafish wild-type *Amotl2*, *Amotl2-ΔPDZ* overexpression in HEK293T cells was able to enhance the ELK1-luciferase reporter expression regardless of FGF2 stimulation (Fig. 6*A*) and to increase the p-ERK1/2 levels (Fig. 6*B*). This implies that Amotl2 promotes MAPK activity independent of the PDZ-binding motif.

We found that 40% (n = 80) of *Tg(fli1:EGFP)*^{y1} embryos injected with *amotl2-ΔPDZ* mRNA exhibited slow migrating of some intersegmental vessels at 36 and 48 hpf (Fig. 6, *E* and *H*) in a way similar to those observed in *amotl2* morphants (Fig. 1, *D* and *E*), whereas almost all embryos injected with *amotl2* mRNA had normal intersegmental vessels (Fig. 6, *D* and *G*). Besides, ~40% of HUVECs transfected with human *AMOTL2-ΔPDZ* were not polarized with scattered distribution of the trans-Golgi marker TGN46 (Fig. 6, *J* and *K*), whereas HUVECs overexpressing wild-type human *AMOTL2* were correctly polarized (Fig. 6, *I* and *K*). However, *Tg(fli1:nEGFP)*^{y7} embryos injected with *amotl2-ΔPDZ* mRNA had endothelial cell number/ISV comparable with that in uninjected or *amotl2* mRNA-injected embryos, as observed at 48 hpf (Fig. 6, *L–O*). Therefore, overexpression of *Amotl2-ΔPDZ* interfered with endothelial polarity but not proliferation.

Amotl2 Regulates FGF/MAPK Signaling through c-Src Depending on Tyr-103 Phosphorylation—Our next question was how Amotl2 regulated FGF-activated MAPK activity. Considering that c-Src is an important mediator of FGF signals and can bind to Amotl2 (13), we hypothesized that Amotl2 might activate MAPK via c-Src. To test this possibility, HEK293T cells transfected with human *AMOTL2* were treated by PP2, an inhibitor of Src kinases (32), with or without FGF2 stimulus.

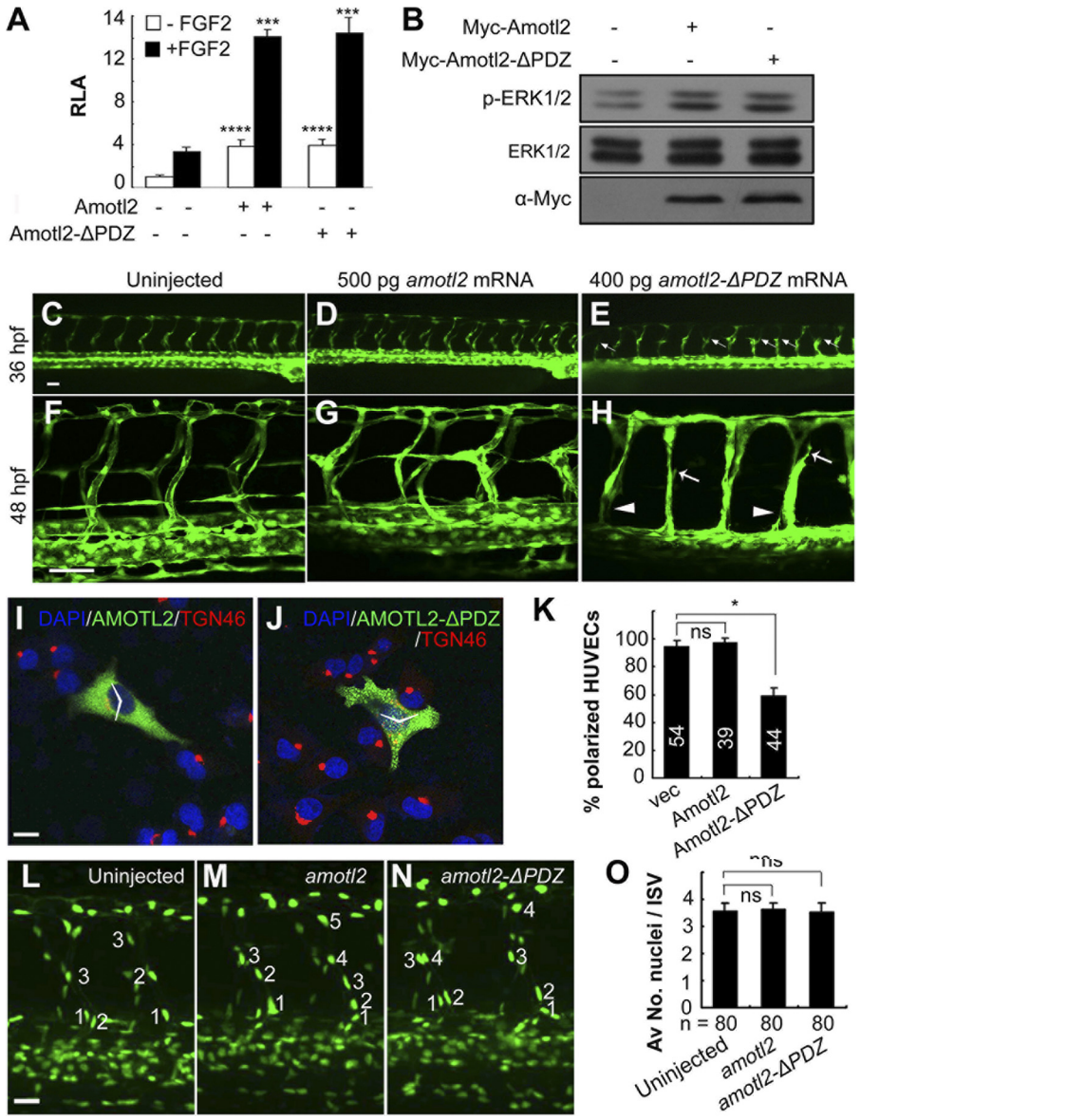

FIGURE 6. **PDZ-binding domain of Amotl2 is involved in ISV growth and cell polarity but not required for MAPK activation and cell proliferation.** *A*, Amotl2 with a loss of its PDZ-binding motif also enhanced ELK1-luciferase reporter expression in HEK293T cells regardless of FGF2 (20 ng/ml) stimulation. Data represent the mean ± S.D. (*error bars*) of triplicates after being normalized to *Renilla* activity. The relative luciferase activity (*RLA*) for transfected cells was compared with that in untransfected cells with significance levels: ***, $p < 0.005$; ****, $p < 0.0001$. *B*, either zebrafish wild-type Amotl2 or mutant Amotl2-ΔPDZ enhanced ERK activation in HEK293T cells. Protein levels were examined by Western blotting using corresponding antibodies after transfection. *C–H*, overexpression of *amotl2-ΔPDZ* inhibited ISV growth in *Tg(fli1:EGFP)*^{y1} transgenic embryos. Trunk regions of embryos at indicated stages were observed by confocal microscopy. *Scale bars*, 75 μm in *C* and 50 μm in *F*. *Arrows* and *arrowheads* indicate slow growing ISVs and ISVs poorly connected to the dorsal aorta, respectively. *I–K*, subcellular location of the Golgi apparatus in HUVECs transfected with Amotl2 or Amotl2-ΔPDZ is shown. Cells were immunostained with TGN46 antibody, and nuclei were labeled with DAPI. *Scale bar*, 20 μm. Statistical data are shown in *K*. *ns*, not statistically significant ($p > 0.01$). *, $p < 0.05$. *L–O*, overexpression of *amotl2-ΔPDZ* mRNA in *Tg(fli1:nEGFP)*^{y1} transgenic embryos had no effect on the number of nuclei in the ISVs. Embryos were injected with 200 pg of *amotl2* or *amotl2-ΔPDZ* mRNA at the one-cell stage and observed at 48 hpf for GFP by confocal microscopy (*L–N*), and the nuclei were counted (*O*). *Scale bar*, 20 μm. *ns*, not statistically significant ($p > 0.001$).

Results showed that PP2 treatment dramatically reduced endogenous p-ERK1/2 levels in untransfected cells as well as *AMOTL2*-transfected cells either in the absence or presence of exogenous FGF2 stimulus (Fig. 7*A*). This suggests that AMOTL2 enhancement of MAPK activation relies on the kinase activity of c-Src; in other words, Amotl2 acts upstream of c-Src in the FGF/Ras/Raf/ERK cascade.

We noted that human, mouse, and zebrafish Amotl2 proteins share a putative YEEA SH2-binding motif within the N-terminal glutamine-rich domain (Fig. 7*B*). This motif with the phosphorylated tyrosine in XB130 protein has been found to be essential for interacting with c-Src (33). The fact that Amotl2 promotes FGF/MAPK signaling provoked us to test whether Tyr-103 of Amotl2 could be phosphorylated by FGF receptor tyrosine kinase activity. As shown in Fig. 7*C*, tyrosine phosphorylation could be detected with an anti-Tyr(P) antibody in HA-Amotl2 immunoprecipitates in HEK293T cells (in *first lane*), which was markedly increased by FGF2 stimulation (in *second lane*). In contrast, tyrosine phosphorylation was absent in immunoprecipitated HA-Amotl2(Y103F) (in *third*

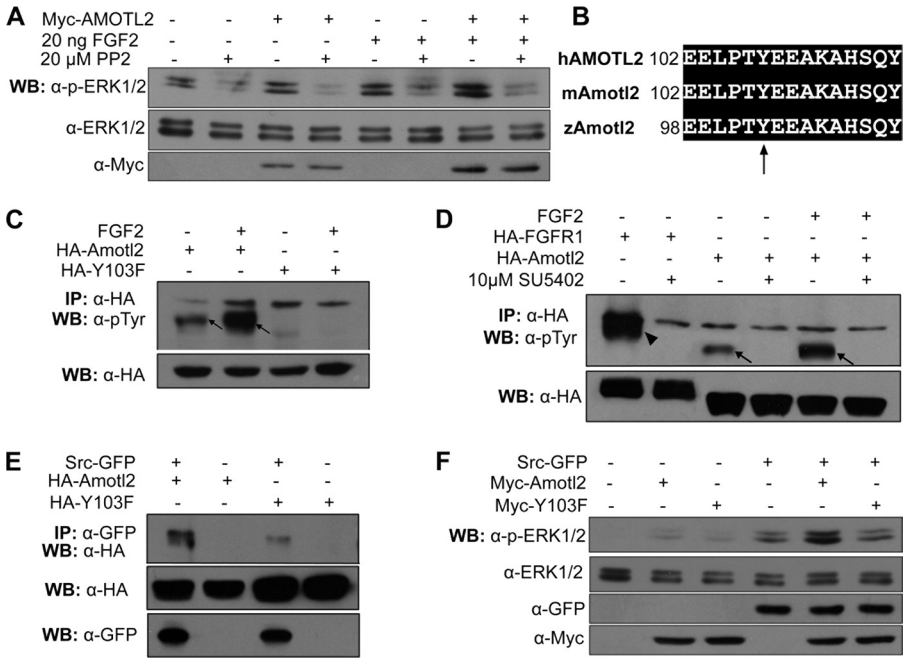

FIGURE 7. **Amotl2 promotes MAPK activation through c-Src depending on its Tyr-103 phosphorylation.** *A*, Amotl2-mediated MAPK activation depended on Src kinase activity in HEK293T cells. Addition of the Src kinase inhibitor PP2 inhibited Myc-AMOTL2-up-regulated p-ERK1/2 levels, as detected by Western blotting (*WB*). *B*, the YEEA SH2-binding motif is conserved among human, mouse, and zebrafish Amotl2. The *numbers* indicate the position of the first residue in the alignment, and the *arrow* indicates the putative tyrosine phosphorylation site. *C*, FGF2 stimulus led to Amotl2 tyrosine phosphorylation at the Tyr-103 site in HEK293T cells. The total phosphotyrosine levels were detected by the anti-phosphotyrosine (*pTyr*) antibody in the immunoprecipitates (*IP*). The tyrosine-phosphorylated Amotl2 band is indicated by *arrows*. *D*, SU5402 inhibited the tyrosine phosphorylation of Amotl2 in HEK293T cells. The tyrosine-phosphorylated FGFR1 band (manifesting effectiveness of SU5402) is indicated by an *arrowhead* and the tyrosine-phosphorylated Amotl2 by *arrows*. *E*, Y103F mutation in zebrafish Amotl2 weakened the interaction between Amotl2 and c-Src in HEK293T cells. HA-Y103F, HA-Amotl2(Y103F). *F*, Tyr-103 mutation in Amotl2 caused a loss of synergistic effect with c-Src on MAPK activation in HEK293T cells.

and *fourth lanes*), a phosphorylation-resistant mutant form of Amotl2, even if FGF2 was applied. Furthermore, FGF2-induced tyrosine phosphorylation of HA-Amotl2 was wholly inhibited by the addition of SU5402 (Fig. 7*D*), an FGF receptor tyrosine kinase inhibitor that efficiently blocked the tyrosine phosphorylation of HA-FGFR1 itself (*second lane* in Fig. 7*D*). These data support an idea that Amotl2 Tyr-103 can be phosphorylated by FGF receptor tyrosine kinase activity.

We then determined whether Amotl2 Tyr-103 is required for its interaction with c-Src. Co-immunoprecipitation analysis showed that the amount of Amotl2(Y103F) associating with Src-GFP markedly reduced (Fig. 7*E*), suggesting a role of Amotl2 Tyr-103 phosphorylation in binding to c-Src. Consistent with this finding, co-transfection of Src-GFP with wild-type Amotl2 (Myc-Amotl2) into HEK293T cells further elevated p-ERK1/2 levels compared with single transfections, whereas the p-ERK1/2 level in cells co-transfected with Src-GFP and Myc-Amotl2(Y103F) was comparable with that in cells transfected with Src-GFP alone (Fig. 7*F*). These results together support the idea that Amotl2 Tyr-103 phosphorylation is important for binding to and synergistically functioning with c-Src to activate the downstream Raf/Ras/ERK pathway.

DISCUSSION

In this study, we uncover a critical function of Amotl2 in angiogenesis. In zebrafish embryos, *amotl2* is required for ISV endothelial migration as well as proliferation. *AMOTL2* in HUVECs also plays important roles in proliferation, polarity, and tube formation. Amotl2 acts to promote MAPK/ERK activation in endothelial cells, which is independent of the PDZ-binding domain.

Previously, Amot and Amotl1 have been shown to promote endothelial cell migration and angiogenesis (7–12). Although Amotl2, the third member of Motin protein family, is expressed in blood vessels in zebrafish embryos (13), its role in vasculature formation is not investigated. In this study, we demonstrate that *amotl2* is required for angiogenesis in zebrafish embryos. So, all three members of Motin family are implicated in blood vessel formation, implying that they all have inherited this function from their common ancestor. However, they may have distinct functions in other cellular and developmental processes.

We demonstrate that Amotl2 positively regulates MAPK/ERK signaling in angiogenic endothelial cells. Our finding conflicts with a previous report that Amotl2 inhibits ERK activation in MCF10A mammary epithelial cells (15). Such a difference may arise from different cell types. We note that Amot has been found to act as a positive regulator of Rac1/MAPK/ERK signaling in HEK293 cells and $Nf2^{-/-}$ Schwann cells (23). It appears that regulation of MAPK signaling by Motin family members is another evolutionarily conserved function for this protein family. We demonstrated previously that Amotl2 can bind to and facilitate translocation of activated c-Src toward the cytoplasm membrane (13). Considering that c-Src participates in FGF/MAPK signaling cascade, we believe that Amotl2 regulate MAPK activation via c-Src. Furthermore, Amotl2 Tyr-103 can be phosphorylated by FGF signals, and this

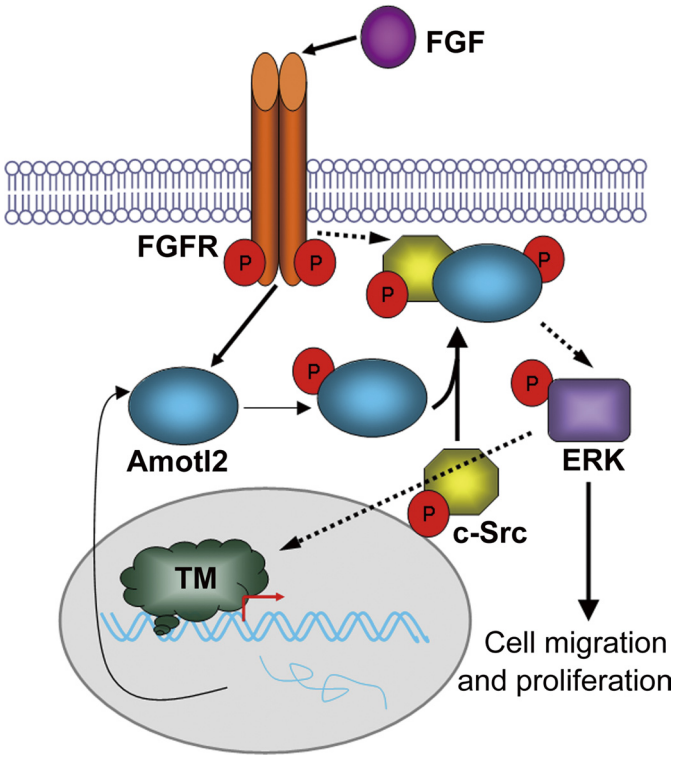

FIGURE 8. **Model for mutual regulation between FGF/MAPK signaling and Amotl2.** FGF signals positively regulate *amotl2* transcription probably through the MAPK cascade; FGF-activated FGFR phosphorylates tyrosine at position 103 of Amotl2; phosphorylated Amotl2 promotes FGF/MAPK signaling by binding to and facilitating translocation of phosphorylated c-Src; finally, MAPK signaling promotes migration and proliferation of endothelial cells. *TM*, transcription machinery.

phosphorylation is important for binding to and synergistically functioning with c-Src to activate the downstream Raf/Ras/ERK pathway. Our current and previous findings together allow us to propose a model showing reciprocal regulation mechanisms between Amotl2 and FGF signals (Fig. 8). In addition to FGF signals, VEGF signals also play important roles in angiogenesis through the MAPK cascade (19, 34). It will be interesting to test whether Amotl2 can mediate VEGF signaling.

Members of Motin protein family all share a common C-terminal PDZ-binding motif (6). Previous studies have well established that Amot and Amot1 play a pivotal role in endothelial migration, which requires their PDZ-binding motif (8, 9, 12, 31, 35, 36). Like the Amot mutant depleted of the PDZ-binding motif (8), overexpression of *amotl2-ΔPDZ* in zebrafish embryos impairs migration of ISV endothelial cells but has little effect on ISV endothelial proliferation. In HUVECs, *AMOTL2-ΔPDZ* overexpression disrupts cell polarity. Thus, the conserved PDZ-binding motif of Motin family members contributes to their conserved function in endothelial migration. It has been reported that the PDZ-binding motif of Amot, Amotl1, and Amotl2 binds to the RhoA GTPase exchange factor protein Syx and regulates RhoA activity at the leading edge of migrating cells (31). Another report indicates that the PDZ-binding motif of Amot helps form the Amot-Rich1-Patj-Pals1-Par3-Cdc42 polarity complex (36). These studies indicate that Motin proteins are involved in regulation of Rho GTPase activity via their PDZ-binding motif in endothelial cells. However, the implication of Motin members in proliferation of endothelial cells has not been reported before. We demonstrate that *Amotl2* is required for ISV endothelial proliferation of zebrafish embryos as well as for proliferation of HUVECs. A previous study shows that knockdown of *amotl1* in zebrafish embryos does not affect the number of ISV endothelial cells (12). This suggests that different members of the Motin family have distinct functions. It will be interesting to test whether Amot possesses activity of promoting endothelial proliferation.

Acknowledgments—We thank Drs. Feng Liu and Jiulin Du for the transgenic fish lines Tg(fli1:EGFP)^{y1} and *Tg(fli1:nEGFP)^{y7}, respectively. We thank Dali Li for technical assistance and members of the Meng Laboratory for helpful discussion and technical assistance.*

REFERENCES

1. Childs, S., Chen, J. N., Garrity, D. M., and Fishman, M. C. (2002) *Development* **129,** 973–982
2. Isogai, S., Lawson, N. D., Torrealday, S., Horiguchi, M., and Weinstein, B. M. (2003) *Development* **130,** 5281–5290
3. Lawson, N. D., and Weinstein, B. M. (2002) *Dev. Biol.* **248,** 307–318
4. Blum, Y., Belting, H. G., Ellertsdottir, E., Herwig, L., Lüders, F., and Affolter, M. (2008) *Dev. Biol.* **316,** 312–322
5. Siekmann, A. F., and Lawson, N. D. (2007) *Nature* **445,** 781–784
6. Bratt, A., Wilson, W. J., Troyanovsky, B., Aase, K., Kessler, R., Van Meir, E. G., Holmgren, L., and Meir, E. G. (2002) *Gene* **298,** 69–77
7. Troyanovsky, B., Levchenko, T., Månsson, G., Matvijenko, O., and Holmgren, L. (2001) *J. Cell Biol.* **152,** 1247–1254
8. Levchenko, T., Aase, K., Troyanovsky, B., Bratt, A., and Holmgren, L. (2003) *J. Cell Sci.* **116,** 3803–3810
9. Levchenko, T., Bratt, A., Arbiser, J. L., and Holmgren, L. (2004) *Oncogene* **23,** 1469–1473
10. Aase, K., Ernkvist, M., Ebarasi, L., Jakobsson, L., Majumdar, A., Yi, C., Birot, O., Ming, Y., Kvanta, A., Edholm, D., Aspenström, P., Kissil, J., Claesson-Welsh, L., Shimono, A., and Holmgren, L. (2007) *Genes Dev.* **21,** 2055–2068
11. Ernkvist, M., Birot, O., Sinha, I., Veitonmaki, N., Nyström, S., Aase, K., and Holmgren, L. (2008) *Biochim. Biophys. Acta* **1783,** 429–437
12. Zheng, Y., Vertuani, S., Nyström, S., Audebert, S., Meijer, I., Tegnebratt, T., Borg, J. P., Uhlén, P., Majumdar, A., and Holmgren, L. (2009) *Circ. Res.* **105,** 260–270
13. Huang, H., Lu, F. I., Jia, S., Meng, S., Cao, Y., Wang, Y., Ma, W., Yin, K., Wen, Z., Peng, J., Thisse, C., Thisse, B., and Meng, A. (2007) *Development* **134,** 979–988
14. Chan, S. W., Lim, C. J., Chong, Y. F., Pobbati, A. V., Huang, C., and Hong, W. (2011) *J. Biol. Chem.* **286,** 7018–7026
15. Wang, W., Huang, J., and Chen, J. (2011) *J. Biol. Chem.* **286,** 4364–4370
16. Zhao, B., Li, L., Lu, Q., Wang, L. H., Liu, C. Y., Lei, Q., and Guan, K. L. (2011) *Genes Dev.* **25,** 51–63
17. Katz, M., Amit, I., and Yarden, Y. (2007) *Biochim. Biophys. Acta* **1773,** 1161–1176
18. Hatano, N., Mori, Y., Oh-hora, M., Kosugi, A., Fujikawa, T., Nakai, N., Niwa, H., Miyazaki, J., Hamaoka, T., and Ogata, M. (2003) *Genes Cells* **8,** 847–856
19. Cébe-Suarez, S., Zehnder-Fjällman, A., and Ballmer-Hofer, K. (2006) *Cell. Mol. Life Sci.* **63,** 601–615
20. Roy, H., Bhardwaj, S., and Ylä-Herttuala, S. (2006) *FEBS Lett.* **580,** 2879–2887
21. Murakami, M., and Simons, M. (2008) *Curr. Opin. Hematol.* **15,** 215–220
22. Presta, M., Dell'Era, P., Mitola, S., Moroni, E., Ronca, R., and Rusnati, M. (2005) *Cytokine Growth Factor Rev.* **16,** 159–178
23. Yi, C., Troutman, S., Fera, D., Stemmer-Rachamimov, A., Avila, J. L., Christian, N., Persson, N. L., Shimono, A., Speicher, D. W., Marmorstein,

R., Holmgren, L., and Kissil, J. L. (2011) *Cancer Cell* **19,** 527–540
24. Jia, S., Ren, Z., Li, X., Zheng, Y., and Meng, A. (2008) *J. Biol. Chem.* **283,** 2418–2426
25. Xiong, B., Rui, Y., Zhang, M., Shi, K., Jia, S., Tian, T., Yin, K., Huang, H., Lin, S., Zhao, X., Chen, Y., Chen, Y. G., Lin, S. C., and Meng, A. (2006) *Dev. Cell* **11,** 225–238
26. Zhang, Y., Li, X., Qi, J., Wang, J., Liu, X., Zhang, H., Lin, S. C., and Meng, A. (2009) *J. Cell Sci.* **122,** 2197–2207
27. Leslie, J. D., Ariza-McNaughton, L., Bermange, A. L., McAdow, R., Johnson, S. L., and Lewis, J. (2007) *Development* **134,** 839–844
28. Singer, S. J., and Kupfer, A. (1986) *Annu. Rev. Cell Biol.* **2,** 337–365
29. Kuida, K., and Boucher, D. M. (2004) *J. Biochem.* **135,** 653–656
30. Eswarakumar, V. P., Lax, I., and Schlessinger, J. (2005) *Cytokine Growth Factor Rev.* **16,** 139–149
31. Ernkvist, M., Luna Persson, N., Audebert, S., Lecine, P., Sinha, I., Liu, M., Schlueter, M., Horowitz, A., Aase, K., Weide, T., Borg, J. P., Majumdar, A., and Holmgren, L. (2009) *Blood* **113,** 244–253
32. Hanke, J. H., Gardner, J. P., Dow, R. L., Changelian, P. S., Brissette, W. H., Weringer, E. J., Pollok, B. A., and Connelly, P. A. (1996) *J. Biol. Chem.* **271,** 695–701
33. Xu, J., Bai, X. H., Lodyga, M., Han, B., Xiao, H., Keshavjee, S., Hu, J., Zhang, H., Yang, B. B., and Liu, M. (2007) *J. Biol. Chem.* **282,** 16401–16412
34. Zachary, I. (2003) *Biochem. Soc. Trans.* **31,** 1171–1177
35. Bratt, A., Birot, O., Sinha, I., Veitonmäki, N., Aase, K., Ernkvist, M., and Holmgren, L. (2005) *J. Biol. Chem.* **280,** 34859–34869
36. Wells, C. D., Fawcett, J. P., Traweger, A., Yamanaka, Y., Goudreault, M., Elder, K., Kulkarni, S., Gish, G., Virag, C., Lim, C., Colwill, K., Starostine, A., Metalnikov, P., and Pawson, T. (2006) *Cell* **125,** 535–548